

# TOWARDS A NON-LINEAR FULL AIRCRAFT MODEL FOR PASSENGER AIRCRAFT LOADS CALCULATIONS

Javon C. Farao<sup>1</sup>, Arnaud G. Malan<sup>2</sup>, Francesco Gambioli<sup>3</sup>

<sup>1</sup>PhD Student

Department of Mechanical Engineering  
University of Cape Town  
Industrial CFD Research Group  
frxjav001@myuct.ac.za

<sup>2</sup>Professor

Department of Mechanical Engineering  
University of Cape Town  
Research Director  
Industrial CFD Research Group  
South African Research Chair in Industrial CFD  
arnaud.malan@uct.ac.za

<sup>3</sup>Technical Skills Leader - Wing

'Loads and Aeroelastics' Department  
Airbus Operations  
BS99 7AR, Bristol, United Kingdom  
francesco.gambioli@airbus.com

**Keywords:** geometrically non-linear structures, quadratic mode shape components, reduced-order models

**Abstract:** This study details the development of a computational full aircraft model (FAM) to assess the non-linear response of an aircraft during an aerodynamic gust. A FAM comprises numerous components viz., the structure, aerodynamics and inertial loads. The focus of this study is to implement a geometrically non-linear reduced-order model (ROM) for the wing and assess its aeroelastic response against standard linear approaches. The NASA common research model (CRM) wing is modeled by three-dimensional Timoshenko beam elements in both the linear and non-linear regime. Linear responses are derived from standard linear modal analysis procedures. The geometrically non-linear beam element ROM is solved via quadratic mode shape components in the modal domain. These components are extracted from linear mode shapes in a novel approach for elastic beam elements. A representative gust load is applied to the structure and the responses are compared to the linear approach. It was found that QMS modal methodology offers improved accuracy by retaining the overall wing length even when loading produces a vertical displacement of 35% with respect to wing span. The extension caused by linear modeling exceeds 14%, while the QMS approach reduces it to less than 3%.

## INTRODUCTION

Commercial aircraft travel is one of the safest forms of transport. This may be attributed to the enforcement of strict safety regulations required during each phase of its construction, especially the design phase [1]. Computational analysis of all the possible design variables i.e.

numerous altitudes, flight velocities and load conditions, is prohibitively costly. This computational cost is exacerbated when high-resolution models for the structure and aerodynamics are adopted. To minimise calculation time, design engineers employ a full aircraft model comprising a reduced-order model (ROM) of the structure that is coupled to calibrated aerodynamic forces and conservative inertial load approximations. The development of ROMs aim to reproduce the dominant characteristics of the phenomena being modeled at a substantially reduced cost.

With regards to the structural ROM, wing structures have historically been designed as extremely stiff, thus a linear model has sufficed. Even though only linear kinematics is encompassed, it performed relatively well when aerodynamic loading induces small wing deflections. However, due to an increase in light-weight, high aspect ratio wing designs with higher flexibility, linear structural responses the linear model is inaccurate. For this purpose, a geometrically non-linear structural model is undergoing large deformations is warranted.

Full-order non-linear finite element and intrinsic models have demonstrated success in mimicking extreme structural deformations and capturing the higher-order kinematics accurately [2, 3]. However, it requires solution of stiffness matrices at each time step, thus increasing the computational cost and implementation complexity. A key consideration during the design phase of the wing and ROM construction is the trade-off between accuracy and computational cost. Therefore, a pragmatic methodology is opted for by extending on current modal analysis techniques. This enables coupling to current aircraft manufacturer procedures via a seamless implementation.

The structural governing equations are derived using Timoshenko beam assumptions in conjunction with elasticity principles. Discretisation is effected via the finite element method (FEM) and transformed to the modal domain utilising linear mode shapes. Extension to the non-linear regime is performed by including the quadratic mode shape (QMS) components as a higher-order term to the linear modal domain response. This QMS inclusion resolves structural non-linearities by compensating for the artificial stretching of beam elements that occur in linear analyses. Typically, quadratic mode shapes are computed via multiple non-linear structural calculations; however, the new strategy employs linear modal analysis to retrieve the QMS components [4]. Extraction of the QMS components was initially derived for truss elements and has been extended to elastic Timoshenko beam elements. It has demonstrated improved accuracy to linear models and comparable results to commercial non-linear software with a negligible effect on computational effort [5].

The main objective of this paper thus aims to demonstrate the impact of extending the structural ROM to compensate for large deformations in a computationally efficient manner. This entails computing the quadratic mode shape components for an elastic beam element and solving the dynamic finite element governing equations in the modal domain. Accurate calculation of the QMS components is verified against an analytical solution. The dynamic methodology is evaluated on a simple cantilever beam which behaves analogously to a wing that experiences highly non-linear behaviour. The procedure will be assessed on an industrial wing undergoing deformation caused by a representative gust. The NASA common research model wing is investigated with effective loads applied onto the beam. Various beam models are implemented enabling comparison of the responses. Novelty in this work is attained via the accurate inclusion of quadratic mode shape components to solve the non-linear response of a structure.

## STRUCTURAL MODEL

Structural reduced-order models (ROMs) typically used in aeroelastic analysis, constitute sequential finite element beam elements. These are commonly known as a beam-stick models and provide a three-dimensional representation of a passenger aircraft wing, as seen in Fig. 1(a). It is a modeling tool that offers a reduction in computational effort compared to a full-order aircraft wing. The structural stiffness and mass properties are derived from a high-fidelity finite element (FE) mesh of the aircraft wing (Fig. 1(b)) via static condensation. Each beam element comprises two nodes with 6 degrees-of-freedom per node, describing 3 translations and 3 rotations, while lumped masses account for the inertial properties of the structure. Resultantly, the beam ROM exhibits analogous responses to the higher-fidelity structure in terms of axial, bending and torsional behaviour.

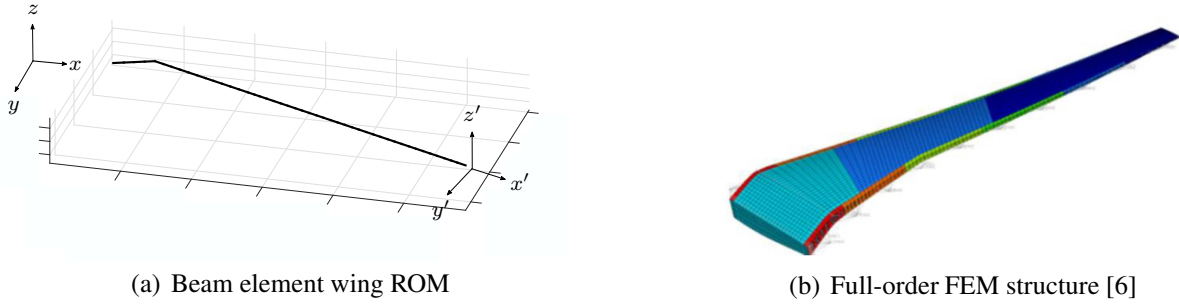


Figure 1: Common research model wing structure: full-order FEM (left) and beam ROM (right)

## Governing equations

The beam element response is governed by Timoshenko beam assumptions which incorporate shear effects and rotary inertia. The governing equations are derived by computing the summation of forces and moments on an infinitesimal Timoshenko beam element, as per Fig. 2. Additionally, elasticity principles, which states that the stresses on an element face should be statically equivalent to the components of the moment and shear force acting upon it, enable completion of the governing equations.

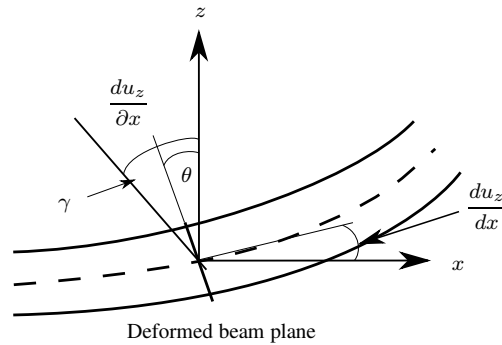


Figure 2: Infinitesimal Timoshenko beam element kinematics during bending

The transient governing equations may thus be stated as follows:

$$\frac{\partial}{\partial x} \left( EI \frac{\partial \theta}{\partial x} \right) + \kappa AG \left( \frac{\partial u_z(x, t)}{\partial x} - \theta \right) - \rho I \frac{\partial^2 \theta}{\partial t^2} = 0 \quad (1)$$

$$\frac{\partial}{\partial x} \left[ \kappa AG \left( \frac{\partial u_z(x, t)}{\partial x} - \theta \right) \right] + q(x, t) - \rho A \frac{\partial^2 u_z(x, t)}{\partial t^2} = 0 \quad (2)$$

where  $E$ ,  $I$ ,  $A$  and  $G$  represents the elastic modulus, area moment of inertia, area and shear modulus of the beam, respectively. The density and shear correction factor is denoted by  $\rho$  and  $\kappa$ . The unknown variables under investigation include the vertical displacement,  $u_z$ , and the rotation of a beam plane,  $\theta$ . Additionally, the translation and torsional balance reads:

$$\frac{\partial}{\partial x} \left[ AE \left( \frac{\partial u_x(x, t)}{\partial x} \right) \right] + b(x, t) = 0 \quad (3)$$

$$\frac{\partial}{\partial x} \left[ GJ \left( \frac{\partial \psi(x, t)}{\partial x} \right) \right] + T(x, t) = 0 \quad (4)$$

Here  $u_x(x, t)$  is the axial displacement and  $\psi(x, t)$  the angular displacement while the axial and torsional forces are defined as  $b(x, t)$  and  $T(x, t)$ . These governing equations are discretised via the finite element method by deploying appropriate shape functions to interpolate the displacement within each element. Accordingly, cubic, hermitian shape functions offer accurate representation of the transverse displacement and rotation at the beam nodes. These variables are interpolated in terms of so-called natural coordinates,  $\xi$ , which run along the beam length as:

$$\begin{aligned} N_{w1} &= \frac{1}{4} (1 - \xi)^2 (2 + \xi) & N_{w2} &= \frac{1}{4} (1 + \xi)^2 (2 - \xi) \\ N_{\theta1} &= \frac{l}{8} (1 - \xi)^2 (1 + \xi) & N_{\theta2} &= \frac{l}{8} (1 + \xi)^2 (1 - \xi) \end{aligned} \quad (5)$$

Linear shape functions are selected to map the axial and torsional variables along the beam with sufficient accuracy, as:

$$N_a = N_t = \left[ \frac{1}{2}(1 - \xi) \quad \frac{1}{2}(1 + \xi) \right] \quad (6)$$

Upon construction of the global governing equations, by summing the individual element contributions, the discrete governing equations is stated as:

$$\mathbf{M}\ddot{\mathbf{U}} + \mathbf{C}\dot{\mathbf{U}} + \mathbf{K}\mathbf{U} = \mathbf{F} \quad (7)$$

Here  $\mathbf{M}$ ,  $\mathbf{K}$  and  $\mathbf{C}$  is the mass, stiffness and damping matrix respectively. The nodal displacement, velocity and acceleration vectors are represented by  $\mathbf{U}$ ,  $\dot{\mathbf{U}}$  and  $\ddot{\mathbf{U}}$ . To enable rapid solution, the time-domain system of equations (Eq. (7)) may be transcribed to the modal form. An eigen-analysis procedure is executed to extract the primary eigen-vectors (mode shapes) that enables the shift to the alternate reference frame. Subsequently, the governing equations are multiplied by a smaller set of linear eigen-vectors, as demonstrated in Eq. (8). This produces a set of decoupled equations of motion in terms of the generalised coordinate,  $\mathbf{q}$ .

$$\Phi^T \mathbf{M} \ddot{\Phi} + \Phi^T \mathbf{C} \dot{\Phi} + \Phi^T \mathbf{K} \mathbf{U} \Phi = \Phi^T \mathbf{F} \quad (8)$$

$$\ddot{\mathbf{q}} + 2\zeta\dot{\mathbf{q}} + \omega^2\mathbf{q} = \mathbf{f} \quad (9)$$

Here,  $\Phi$  denotes the matrix of primary eigen-vectors while  $\omega$  and  $\zeta$  is the natural frequency of vibration and damping ratio, respectively. The subsequent transient analysis is solved via the implicit Newmark method due to its second-order accuracy and stability characteristics [7]. However, prior to dynamic analysis the damping matrix,  $\mathbf{C}$ , is required. For this purpose, Rayleigh proportional damping is utilised due to its ability to preserve the orthogonality of the modes of vibration. The damping matrix is therefore represented as a linear combination of the mass and stiffness matrix, as seen in Eq. (10). Additionally, proportional damping assumes that the eigen-vectors,  $\phi_i$ , are orthogonal to the damping matrix, as shown in Eq. (11).

$$\mathbf{C} = \alpha\mathbf{M} + \beta\mathbf{K} \quad (10)$$

$$\phi_i^T \mathbf{C} \phi_j = 2\omega_i \zeta_i \delta_{ij} \quad (11)$$

The scalar coefficients  $\alpha$  and  $\beta$  are derived from the orthogonality of the damping matrix, by substituting Eq. (10) into Eq. (11). The coefficients are thus determined from the specified modal damping ratios  $\zeta_1$  and  $\zeta_2$ , which correspond to the first and second modes respectively. Damping is a phenomenon which should be applied so as to describe the physics specific to a particular structure. Taking cognisance of this, a minimum damping of 2% is required, which translates to  $\zeta_1 = \zeta_2 = 0.02$ . Subsequent to solution of generalised coordinates, the linear time-domain response is computed by multiplication with linear mode shapes, as follows:

$$\mathbf{U}(x, t) = \sum_i q_i \phi_i \quad (12)$$

Extending it to the geometrically non-linear regime is enacted by including the quadratic mode shape components,  $\mathbf{G}_{ij}$ , into the transformation to the time-domain, as per Eq. (13) [8]. The quadratic mode shape components are generally calculated from multiple non-linear static analyses. However, due to the computational cost implications of such an endeavour, a methodology was proposed that employs the linear eigen-vectors to produce accurate quadratic mode shape components for truss elements [9]. The authors of this paper have extended on this approach, thus enabling extraction of QMS components for elastic beam elements. This novel work offers marked improvements in accuracy of the structural transient response when compared to existing linear models. Moreover, minimal additional complexity or computational overhead is generated during the analysis.

$$\mathbf{U}(x, t) = \sum_i q_i \phi_i + \sum_i \sum_j q_i q_j \mathbf{G}_{ij} \quad (13)$$

### Quadratic mode shape components

Applying linear modal methods to dynamic analysis cause the endpoints of a beam element to translate in a straight line during deformation. The limitation of linear kinematics produces a linear trajectory of the endpoints under rotation, as demonstrated by the red line in Fig. 3. This results in a non-physical extension of the element. The derivation of the quadratic beam mode shape thus aims to compensate for the artificial stretching. This would result in a trajectory closer to the green, curved line in the figure.

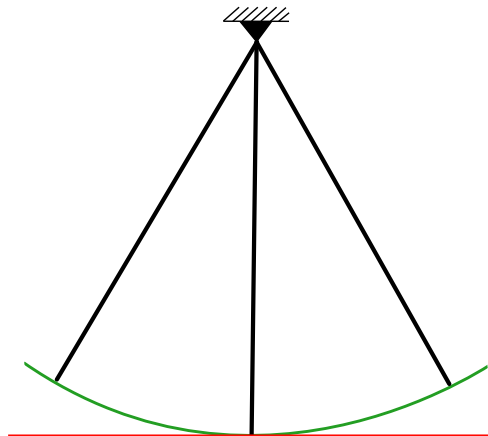


Figure 3: Beam tip trajectory due to rotation via linear (red) and non-linear analysis (green)

The process to compute the QMS components of an elastic beam element may be summarised as follows:

- Account for the stretching of a node relative to a reference point in each mode by appending a quadratic term containing the quadratic mode shape components. This may be computed accordingly as:

$$s_n = q_i (\mathbf{u}_i^{e,2} - \mathbf{u}_i^{e,1}) \cdot \mathbf{l}_e / l_e^2 + \frac{1}{2} q_i^2 \mathbf{R}_e^2 \mathbf{l}_e + q_i^2 (\mathbf{G}_{ij}^{e,2} - \mathbf{G}_{ij}^{e,1}) \cdot \mathbf{l}_e / l_e^2 \quad (14)$$

where  $\mathbf{l}_e$  denotes the element length vector and  $\mathbf{R}_e$  is the element rotation matrix in a mode shape. Moreover,  $\mathbf{u}_i^{e,n}$  symbolises the displacement of node  $n$  in element  $e$  for a specific mode,  $i$ .

1. Place a reference point,  $\mathbf{P}_r$ , at the midpoint of the beam element in a specific deformed modal orientation.
2. Determine the higher-order rotation of an element due to each mode shape

$$\mathbf{R}_e^i = \mathbf{l}_e \times (\mathbf{u}_i^{e,2} - \mathbf{u}_i^{e,1}) / l_e^2 \quad (15)$$

3. Calculate the artificial stretching at each node due to the element's rotation

$$\mathbf{s}_n = \frac{1}{2} [\mathbf{R}^i \times (\mathbf{R}^j \times \mathbf{d}_n) + \mathbf{R}^j \times (\mathbf{R}^i \times \mathbf{d}_n)] \quad (16)$$

Here,  $\mathbf{d}_n$  denotes the vector from the reference point,  $\mathbf{P}_r$ , to the beam element end-node.

- Multiply the higher-order stretching for that mode contribution by the element's local stiffness matrix,  $\mathbf{K}_l$ , to compute an associated force.

$$\mathbf{f}_n = \mathbf{u}_n \mathbf{K}_l \quad (17)$$

Performing a summation of forces over the nodes results in a linear static problem. Additionally, a Lagrange multiplier,  $\lambda$ , is included into the force summation because the system of equations may be solved via partial inversion as follows:

$$\mathbf{F} = \mathbf{K} \mathbf{G}_{ij} + \lambda \mathbf{K} \phi_i \quad (18)$$

- Ensure orthogonality is conserved between the linear and quadratic mode shapes with respect to the stiffness matrix as follows:

$$\phi_i^T [\mathbf{K}] \mathbf{G}_{ij} = 0 \quad (19)$$

Solving Eq. (18) and Eq. (19) simultaneously for each mode combination yields the quadratic mode shape vector.

## EVALUATION AND VERIFICATION

### Analytical solution

Employing the aforementioned algorithm produces a QMS vector,  $\mathbf{G}_{ij}$ , due to a combination of 2 linear mode shape pairs,  $\phi_i$  and  $\phi_j$ . This vector contains components that compensate for the stretching of the element in each mode. Therefore, it contains the QMS component that represents the horizontal deflection,  $\Delta x$ , induced during non-linear deformations, as seen in Fig. 4. These components are verified against an analytical expression for the lateral deflection, as illustrated in Eq. (20) [8]. The axial displacement,  $\Delta x$ , preserves the length of the structure ensuring a geometrically non-linear response is produced. The complex cantilever mode shape (Eq. (21)) and its spatial derivative is denoted by  $\phi_i$  and  $\phi'_i$ , respectively. The product of  $\lambda l$  refers to the first 4 characteristic natural frequencies of the beam.

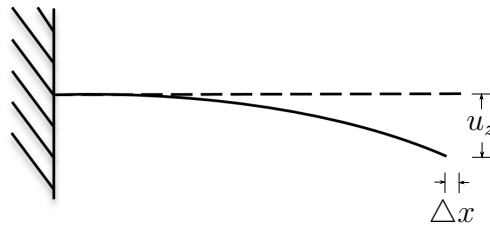


Figure 4: Undeformed and non-linear deformed beam configurations under tip loading

$$\mathbf{G}_{ij} = -\frac{1}{2} \int_0^l (\phi'_i \phi'_j) dx = -\Delta x \quad (20)$$

$$\phi_i = \sin(\lambda x) - \sinh(\lambda x) + \alpha_n (\cosh(\lambda x) - \cos(\lambda x)) \quad (21)$$

$$\alpha_n = \frac{\sin(\lambda l) + \sinh(\lambda l)}{\cos(\lambda l) + \cosh(\lambda l)} \quad (22)$$

$$\lambda l = 1.875; 4.694; 7.8548; 10.9955 \quad (23)$$

The beam element properties are listed as follows: elastic modulus of 200 GPa, density of  $7800 \text{ kg/m}^3$ , length of 20 m and a cross-sectional area of  $7.854 \times 10^{-5} \text{ m}^2$ . The beam structure is compared against a cantilever truss network (Fig. 5(a)) with the same properties, yet the beam consists of 66 degrees-of-freedom (dofs) while the truss network comprises of 164 dofs.

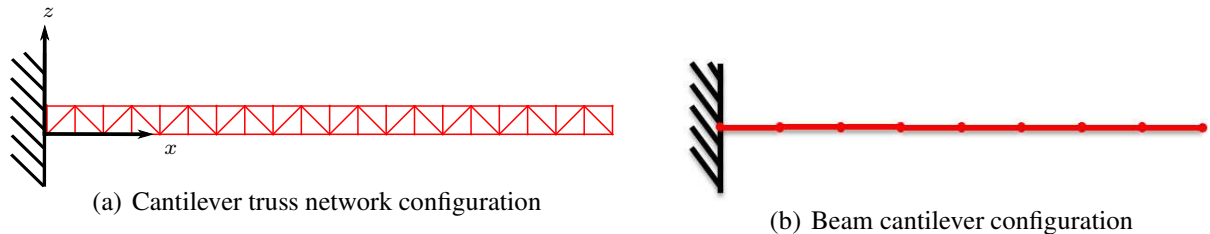


Figure 5: Cantilever configurations for comparison: truss network (left) and beam structure (right)

The first 3 linear mode combinations are utilised to compare the QMS components for the beam and truss cantilever configurations against the analytical results, as shown in Table 1. Even though the beam structure contains over 50% fewer dofs, the beam configuration provides greater accuracy compared to the truss network. This result proves that the extension of the methodology to beam elements is accurate. Consequently, the aim is to ascertain the validity of QMS components in non-linear transient analysis.

Mode contributions		Analytical	Truss Structure		Beam Structure	
$i$	$j$		Numerical	% error	Numerical	% error
1	1	-0.02905	-0.02887	0.62	-0.02904	0.01
1	2	-0.04612	-0.04683	1.53	-0.04612	0.00
1	3	-0.02463	-0.02242	9.01	-0.02463	0.00
2	2	-0.20261	-0.21217	4.72	-0.20246	0.07
2	3	-0.13970	-0.14268	2.13	-0.13970	0.00
3	3	-0.48312	-0.54488	12.78	-0.48193	0.25

Table 1: Comparison of QMS components of truss and beam structures to analytical

### Non-linear transient analysis

The non-linear modal methodology is assessed against a geometrically non-linear time-domain model computed by the commercial code, MSC Nastran. The beam is excited by a constant vertical tip force that is large enough to invoke non-linear deformations viz.,  $F = 10kN$ . This corresponds to a normalised load factor of  $\kappa = \frac{FL^3}{EI} = 1.0$  as illustrated in Fig. 6(b) (red cross). The figure plots the normalised load factors vs. deflection ratio for geometrically linear and non-linear cantilever beams (Fig. 6(a)) due to dynamic loading conditions. A deflection ratio of  $\frac{u_z}{l} \approx 0.4$  is found to be sufficient for valid non-linear comparisons. Structural damping is neglected and out-of-plane displacements ( $z$ -displacements) remain unaffected.

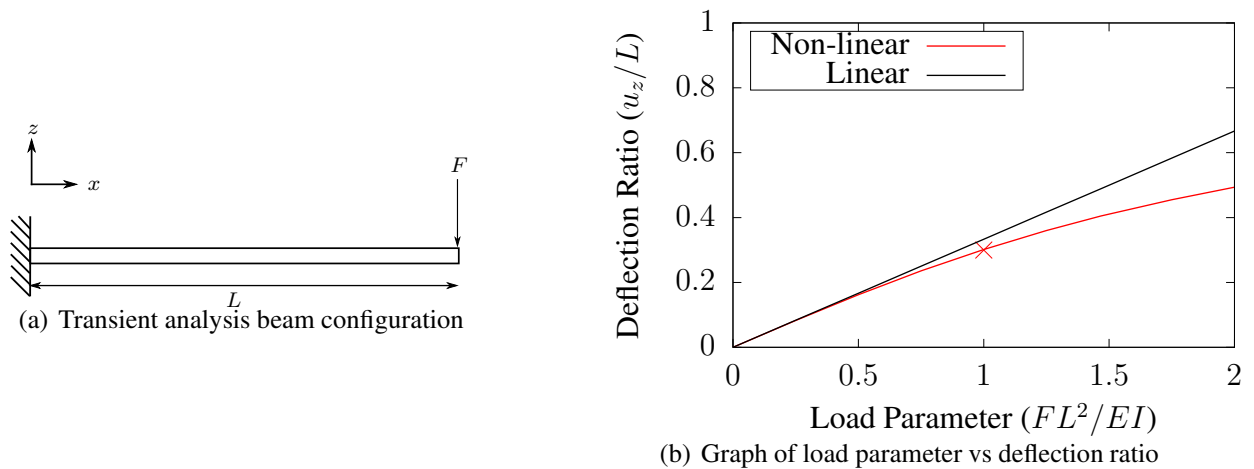


Figure 6: Boundary conditions for transient analysis (left) and extent of load applied onto beam structure (right)

The dynamic response of the beam is computed via the proposed modal procedure by including the linear and quadratic mode shape components, as per Eq. (13). It was found that extending the linear modal analysis to include quadratic mode shapes in elastic elements requires minimal additional computational effort. In contrast, Nastran currently employs a high-fidelity approach for non-linear dynamic analysis which computes the structural response via the Newton Raphson method [10]. This procedure is costly due to it calculating the stiffness matrix at each iteration. Comparison of the beam tip displacement computed via linear modes, QMS components and non-linear time-domain is illustrated in Fig. 7.



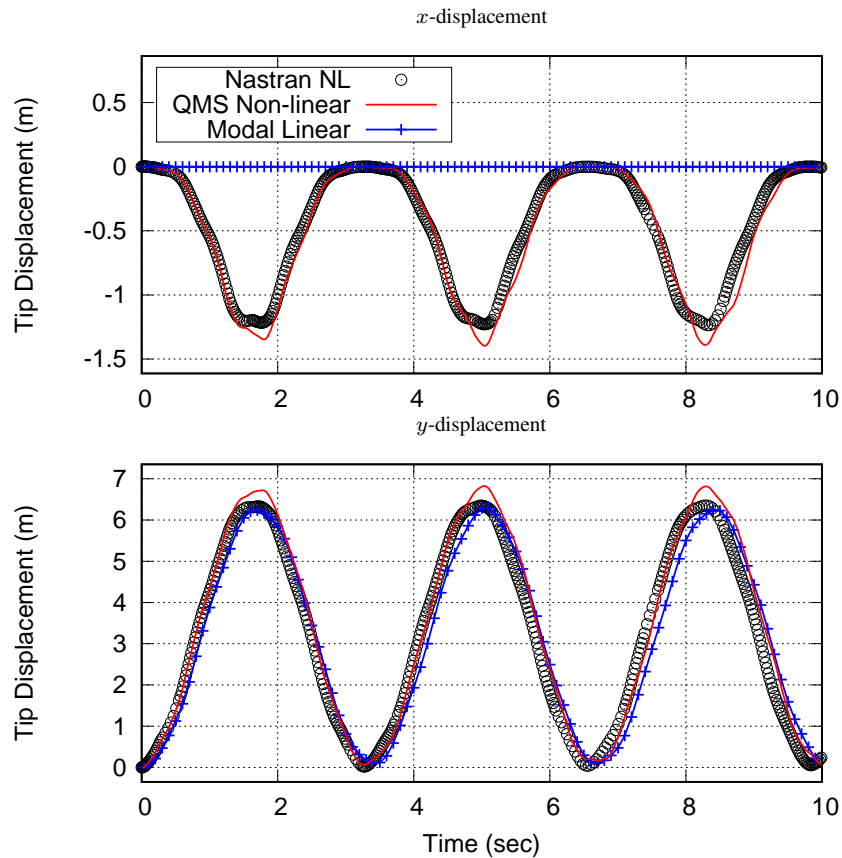


Figure 7: Comparison of non-linear dynamic response of beam tip via various analysis methods

As can be seen in Fig. 7, the QMS analysis provides an accurate approximation to the non-linear Nastran solution in both  $x$ - and  $y$ -directions. The difference between the linear and non-linear case is seen in the movement of the beam tip toward the fixed constraint. Existence of  $x$ -displacements as the beam deflection increases proves that a spatial non-linear transient response is present. The amplitude provides good correspondence nonetheless with the maximum peak-to-peak error being 7% for a time-independent solution.

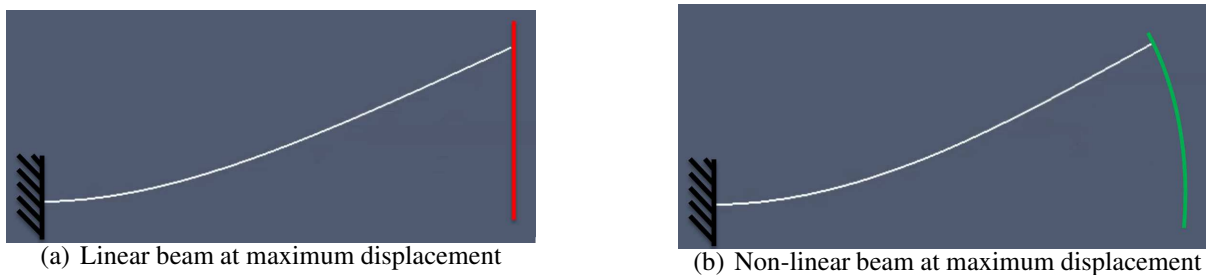


Figure 8: Linear (left) and non-linear (right) dynamic response at  $t = 3\text{sec}$  (unscaled displacement)

Animation snapshots of the linear and non-linear overall beam response is shown in Figs. 8(a) and 8(b). The linear structure beam tip moves in a straight vertical line (red line), resulting in element stretching. In contrast, the QMS non-linear analysis allows the beam tip to move in a parabolic locus (as shown by the green curve) which preserves the beam length to a much greater degree. A comparison between the change in length of the linear and the non-linear analysis is shown in Fig. 9. The QMS non-linear solution, with an extension error of only 0.4%, provides a significant improvement to the linear analysis, which bears an error of 6.3%.

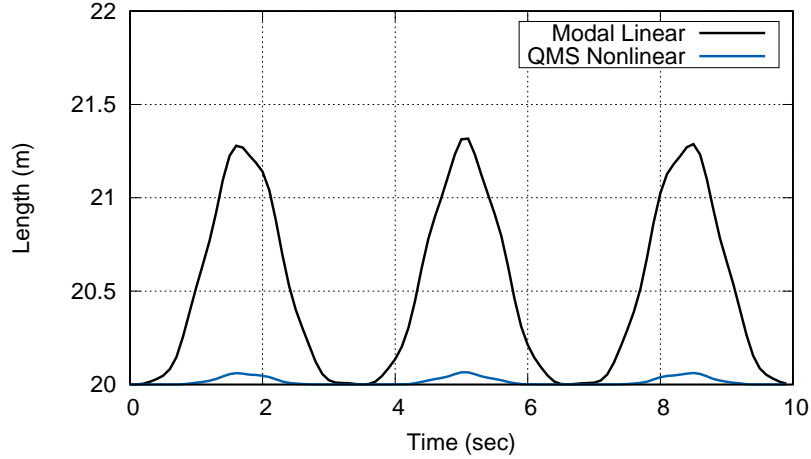


Figure 9: Comparison of change in cantilever beam length between linear and QMS non-linear analyses

### Industrial application

The developed non-linear modeling technology is next applied to a structural ROM of an actual aircraft wing for further verification. For this purpose, the NASA (CRM) [6] wing is employed. The full order FE model is depicted in Fig. 1(b). Standard static-condensation produces a complex structure, thus a manual condensation process is performed to extract an analogous beam element with properties at span-wise sections<sup>1</sup>. Similarly, point masses were placed at the beam nodes to mimic the full-order model. The resulting beam ROM (Fig. 1(a)) was subjected to a modal analysis to determine the precision of the eigen-values in comparison to the full scale model. The values were found to be within 10% which is deemed sufficient for the purposes of this investigation.

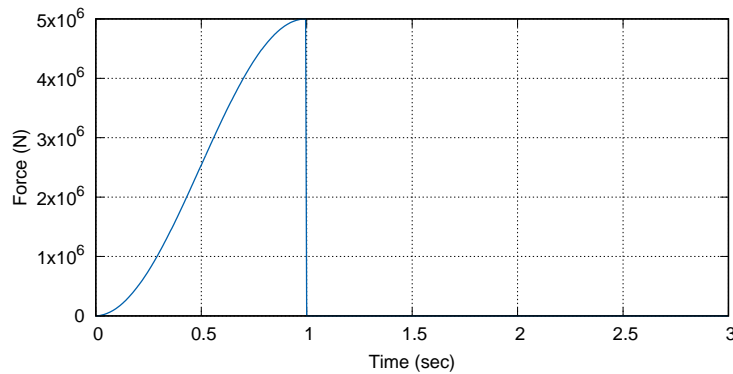


Figure 10: CRM wing ROM tip force (z-direction)

Boundary conditions are applied by fully constraining the wing ROM at the wing root-fuselage connection i.e., kink in Fig. 1(a). A vertical tip load ( $z$ -direction) is applied to the beam tip and represents half a sinusoidal gust peaking after 1 second (Fig. 10). The load is given an amplitude of  $5 \times 10^6 \text{ N}$  to elicit large displacements. Structural damping is set to 2% of the first two modes via Rayleigh damping (Eq. (10)). The non-linear transient response of the wing is determined through a systematic analysis process, where the QMS components are computed and included in the dynamic analysis (Eq. (13)).

<sup>1</sup>This was performed by Dr. R. Cook from the University of Bristol

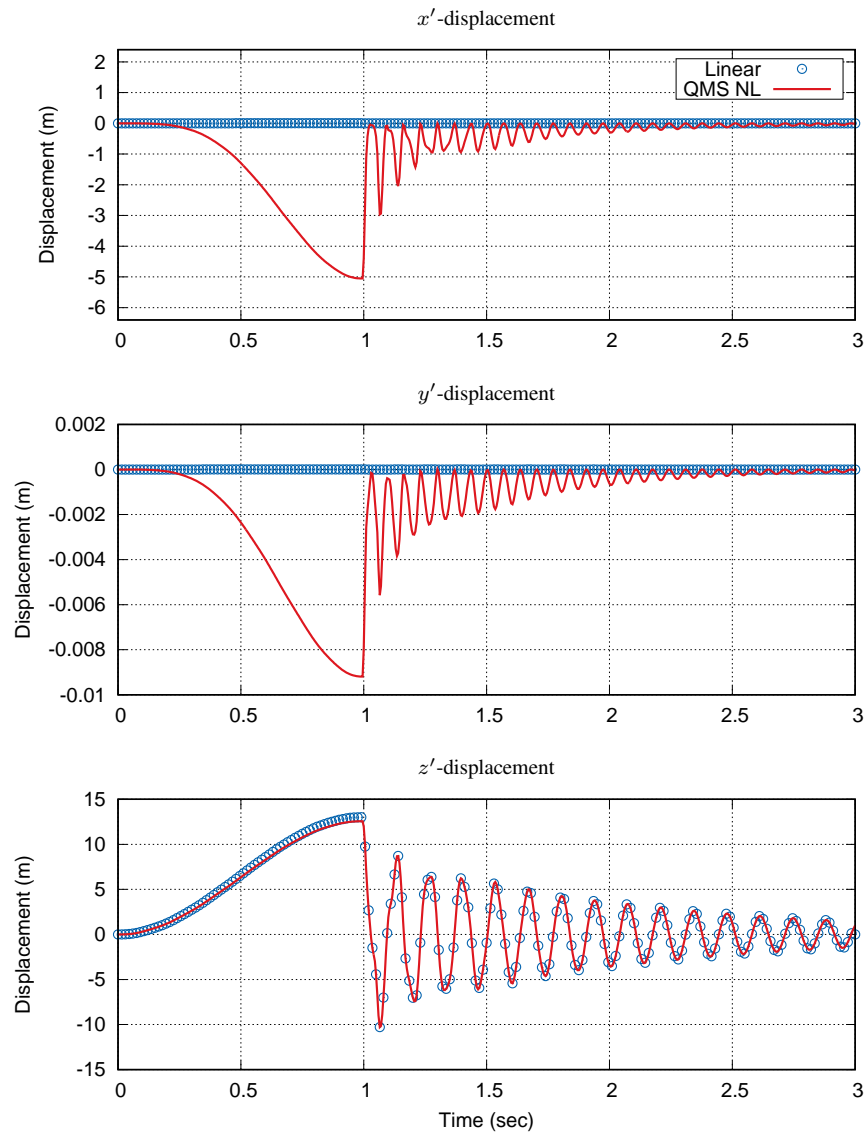


Figure 11: CRM wing tip displacement in local coordinates due to linear and QMS non-linear (NL) analyses

As can be seen in Fig. 11, the linear beam tip exhibits no displacements in the direction along the beam,  $x'$ -direction, while the non-linear QMS result displays axial deflection. Due to the load inducing a vertical displacement larger than 35% of the wing length, axial displacements are expected. The out-of-plane displacements ( $y'$ -axis) arise due to the CRM wing not being exactly on the  $x'$ -axis. These offset values, albeit slight, cause the relatively small out-of-plane oscillation. Although it is difficult to glean the accuracy of the results via a sole comparison to the linear solution, the length preservation of the wing is used to illustrate the improvement in accuracy. The beam extension error resulting from linear analysis is 13.05% while the non-linear QMS only exhibits a 2.89% error.

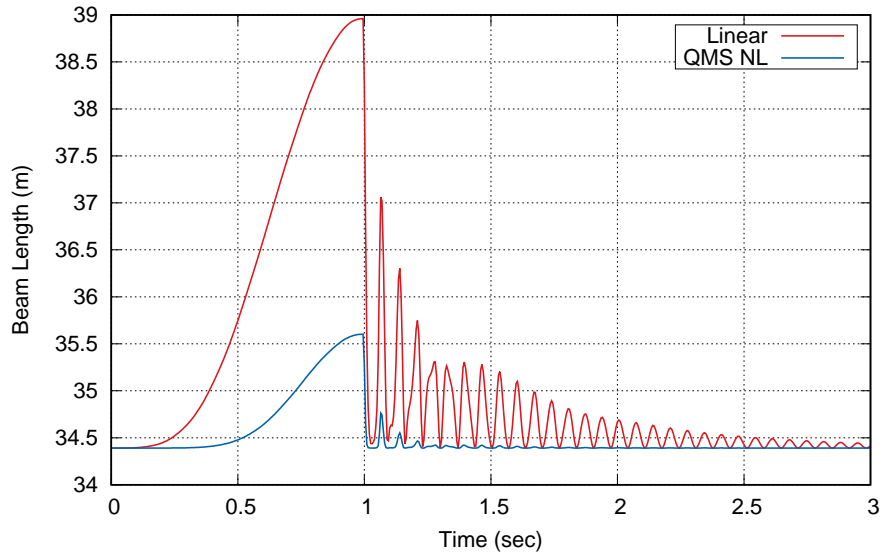


Figure 12: Linear and QMS beam length change during the simulation

## CONCLUSION

A robust and efficient geometrically non-linear finite element beam structure is constructed by including quadratic mode shape components. These components, initially derived for truss elements via linear modal analysis, are extended to and assessed on elastic beam elements. Comparison of various element structures to the analytical non-linear eigen-vector proves that beam elements are superior with an 11% increase in accuracy. With regards to the transient analysis, the quadratic modal analysis of a cantilever beam ROM exhibits accurate approximations to commercial software with a tip displacement amplitude error of only 7%. The higher-order kinematics are also captured appropriately with points vibrating along a curved path. Resultantly, the structural length is conserved up to 3 times better than the linear regime. The methodology was successfully applied to an industrially relevant 3-dimensional wing ROM viz., the NASA common research model wing. Overall, this methodology demonstrates drastic improvements to current methods at a fraction of the computational effort required of high-fidelity solvers.

## ACKNOWLEDGMENTS

Part of the research leading to this work was supported by the AEROGUST project (funded by the European Commission under grant agreement number 636053). The partners in AEROGUST are: University of Bristol, INRIA, NLR, DLR, University of Cape Town, NUMECA, Optimad Engineering S.r.l., University of Liverpool, Airbus Defence and Space, Dassault Aviation, Piaggio Aerospace and Valeol. It was additionally supported by the 'Loads and Aeroelastics' Department of Airbus Operations in Bristol (UK) and the National Aerospace Centre (NAC) of South Africa. Special thanks also goes to Dr. R. Cook of Bristol University who produced the beam properties of the CRM wing.

## REFERENCES

- [1] EASA (2015). Acceptable means of compliance for large aeroplanes. cs-25. Tech. rep., European Aviation Space Agency.
- [2] Bathe, K.-J. and Bolourchi, S. (1979). Large displacement analysis of three-dimensional beam structures. *International Journal for Numerical Methods in Engineering*, 14(7), 961–986.
- [3] Hodges, D. H. (1990). A mixed variational formulation based on exact intrinsic equations for dynamics of moving beams. *International journal of solids and structures*, 26(11), 1253–1273.
- [4] Segalman, D. and Dohrmann, C. (1996). A method for calculating the dynamics of rotating flexible structures, part 1: Derivation. *Journal of Vibration and Acoustics*, 118(3), 313–317.
- [5] Farao, J. C., Malan, A. G., and Gambioli, F. (2016). A non-linear modal methodology for cantilever beams with application to aircraft structures. *Journal of Aircraft*. Submitted and under review.
- [6] NASA common research model. <http://commonresearchmodel.larc.nasa.gov/>. Accessed: 2017-05-30.
- [7] Bathe, K.-J. (2008). *Finite element method*. Wiley Online Library.
- [8] Robinett III, R. D., Wilson, D. G., Eisler, G. R., et al. (2005). *Applied dynamic programming for optimization of dynamical systems*, vol. 9. Siam.
- [9] Van Zyl, L. and Mathews, E. (2012). Quadratic mode shape components from linear finite element analysis. *Journal of Vibration and Acoustics*, 134(1), 014501.
- [10] Nastran, M. (2014). Basic dynamic analysis user's guide. *MSC. Software Corporation. USA*, 546.

## COPYRIGHT STATEMENT

The authors confirm that they, and/or their company or organization, hold copyright on all of the original material included in this paper. The authors also confirm that they have obtained permission, from the copyright holder of any third party material included in this paper, to publish it as part of their paper. The authors confirm that they give permission, or have obtained permission from the copyright holder of this paper, for the publication and distribution of this paper as part of the IFASD-2017 proceedings or as individual off-prints from the proceedings.